Light propagation in an imperfect photonic crystal

L. Braginsky*
Institute of Semiconductor Physics, 630090 Novosibirsk, Russia

V. Shklover
Laboratory of Crystallography, ETH Zürich, 8093 Zürich, Switzerland
(Received 26 October 2005; published 13 February 2006)

The envelope function approach for the electric and magnetic fields of the light wave in the photonic crystals has been used to investigate the propagation of light in disordered photonic crystals and its reflection or refraction at the boundary. We showed that small long-range distortion of the crystal lattice can explain peculiarities of the transmittance spectrum of the polystyrene colloid film we have grown.

DOI: 10.1103/PhysRevB.73.085107 PACS number(s): 42.70.Qs, 78.67.−n, 42.25.−p, 82.70.Dd

I. INTRODUCTION

Photonic crystals provide a powerful tool for manipulating and controlling of light in three dimensions of space. Nanotechnology may be considered as a promising photonic technology, which can be used for template assisted self-assembly of the microlenses arrays,[1] fabrication of nanoapertures for mapping of the transmitted light,[2] the assembling photoactive antenna (semiconductor nanocore) arrays,[3] direct-writing electron-beam lithography for fabrication of thin-film Ni-O-Ni diode-antenna structures,[4] etc.

Photonic crystals of spherical nanoparticles are usually produced by the self-assembly or lithography techniques. Different combinations of these methods are also possible.[5] Lithography permits formation of the crystal structures of different symmetry, which determines by the substrate. Self-assembly of spherical particles usually results in 3D close packing (fcc or hcp structures), whereas more complicated structures also can be grown. It is important that the lattice constants of all photonic crystals are comparable with the size of the particles their comprising. At the same time, dispersion of the particles sizes, which is inevitable for the artificial "atoms," leads to imperfection of the photonic crystals. This is the main point that distinguishes the photonic and common crystals. The latter comprise of identical atoms that occupy rather small part of the lattice volume.

The problem of the light propagation in the perfect photonic crystals can be solved numerically. Translational symmetry of crystals considerably simplifies the problem, because in this case the Bloch theorem holds.[6] Solution of the Maxwell equations for the light fields in the crystal lattice yields the photonic band structure, which was calculated for the perfect photonic crystals of different symmetries.[7] This allows one to estimate the transmission spectra of the finite photonic crystal layers and compare the results with experiments.[8–10] It has been established that positions of dips in these spectra are usually in accordance with the contemporary theory; however, the dips are essentially wider and their depth is a few orders of value less than that predicted by the theory. We believe that this discrepancy is due to imperfection of the real photonic crystals.

The problem of light propagation in the imperfect photonic crystals is much more complicated, because even small disorder disturbs the translational symmetry; this violates the Bloch theorem making difficulties for the numerical consideration. To cope with this problem, we employ the envelope function approach (EFA), which is commonly used in the solid state theory for investigation of the electron properties. EFA permits dividing the problem into two parts: (1) determination of the photonic band structure of the perfect crystal and (2) investigation of the influence of imperfection or small disorder on the photon transport. The first problem should be considered numerically;[6,7] the results of such calculations can be expressed in terms of the gap values and effective speeds of light in the appropriate photonic bands. These values can be used then as the phenomenological parameters for solution of the second problem; this considerably simplifies the numerical consideration of the problem and permits its analytical analyzing for the small or smooth imperfections.

To study the reflection or refraction of light at the crystal boundary, we have to apply the boundary conditions to the effective electric and magnetic fields. In the optics of common crystals this procedure leads to the well-known Fresnel equations. Derivation of these equations assumes the dielectric permittivity as the smooth function on a scale of the wavelength.[11] This is possible, if the wavelength of light much exceeds the lattice constant of the crystal. This is the case of the common crystals, but not the photonic crystals, the lattice constant of which is comparable with the photon wavelength. To avoid this difficulty, the authors of Ref. 12 used the dynamic scattering theory that has been developed for investigation of the x-ray scattering at the crystal surface. This theory supposes that electric field does not change essentially on a scale of an atom. This is the case of the common crystals, but not the photonic crystals, which "atoms" are of the size comparable with the wavelength of light.

The EPA for the Maxwell equations has been suggested in the papers,[13–17] where this approximation has been used to study the influence of the point defects on the optical properties of PC,[13,14] optical properties of the photonic heterostructures,[15,16] and waveguides.[16,17] In this paper we use the EPA to consider the influence of the extensive defects on the light propagation in the photonic crystals. We obtain the boundary conditions for these envelopes at the boundaries between photonic crystals and photonic crystal—

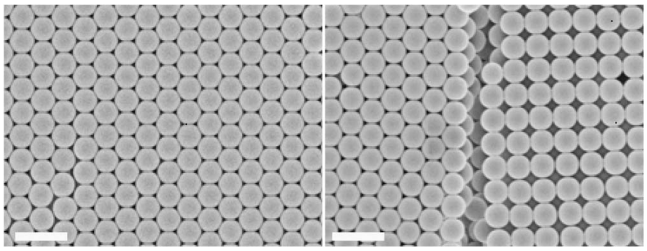

FIG. 1. Examples of photonic crystals, fabricated from the colloidal polystyrene spheres with diameter 404 nm (SEM patterns). Left: a homogeneous crystal with the top (111) surface parallel to the substrate. Right: a nonhomogeneous crystal build of two kinds of domains with the top surfaces (111) and (100) parallel to the substrate. Note that the homogeneous crystal as well as different domains of the nonhomogeneous crystal have the same ccp structure. Scale bar is 1 μm.

vacuum, taking into account existence of the intermediate region at the boundary where one crystal order changes into another. The approach is used to investigate the transmittance of the photonic crystal film.

II. SAMPLE PREPARATION

The shear-flow crystallization method developed by the group of Xia (see, for example, Ref. 18) has been used for fabrication of the metal, metal oxide, and polymer photonic crystals. Typical examples of the fabricated structures are presented in Fig. 1. The structure and optical properties of the films including transmission spectra and band gap structure were reported.[19]

III. ENVELOPE FUNCTION APPROXIMATION FOR THE LIGHT FIELDS IN PHOTONIC CRYSTALS

A. Equation

Let us consider a photonic crystal lattice composed of equal beads, the dielectric permittivity of which is different from that of the surrounding media. For the sake of simplicity we assume both materials as isotropic and the lattice as cubic. The electric field $\boldsymbol{E}(\boldsymbol{r})$ of the light wave obeys the equation

$$\Delta \boldsymbol{E}(\boldsymbol{r}) + \omega^2[\varepsilon(\boldsymbol{r}) + \epsilon(\boldsymbol{r})]\boldsymbol{E}(\boldsymbol{r}) = 0, \tag{1}$$

where ω is the frequency of the light, the permittivity $\varepsilon(\boldsymbol{r})$ is a periodical function of the position $\boldsymbol{r}$, and $\epsilon(\boldsymbol{r})$ is its nonperiodical addition caused by irregularity. We adopt the units where the speed of light in vacuum is equal to unity ($c=1$), otherwise the substitution $\omega \to \omega/c$ has to be done.

The Eq. (1) with $\epsilon(\boldsymbol{r})=0$ leads to the eigenvalue problem that was numerically solved in Ref. 7. The electric field of the wave propagating along the wave vector $\boldsymbol{k}$ obeys the equation

$$\Delta E^{\tau}_{\boldsymbol{k},n}(\boldsymbol{r}) + \omega_n^2(\boldsymbol{k})\varepsilon(\boldsymbol{r})E^{\tau}_{\boldsymbol{k},n}(\boldsymbol{r}) = 0. \tag{2}$$

Here $E^{\tau}_{\boldsymbol{k},n}(\boldsymbol{r})$ is a Bloch function of the nth band, $\omega_n(\boldsymbol{k})$ is the frequency of this band, and $\tau=1,2$ is the polarization index. In general, the frequency $\omega_n(\boldsymbol{k})$ also depends on polarization, and a more complicated operator should replace Δ in Eq. (2); this is not the case for the crystals of cubic symmetry we are considering. The Bloch functions can be normalized as

$$\int_{\mathcal{V}} \varepsilon(\boldsymbol{r}) E^{\tau*}_{\boldsymbol{k},n}(\boldsymbol{r}) E^{\tau'}_{\boldsymbol{k}',n'}(\boldsymbol{r}) d^3\boldsymbol{r} = M \delta_{n,n'} \delta_{\tau,\tau'} \delta_{\boldsymbol{k},\boldsymbol{k}'},$$

where $\mathcal{V}$ is the unit cell, $M=4\pi\hbar\omega_n(\boldsymbol{k})N_{\mathrm{ph}}$, and N_{pn} is the number of photons in the unit cell. We can introduce the Wannier functions $W^{\tau}_n(\boldsymbol{r}-\boldsymbol{R}_i)$, localized at the ith site as follows

$$E^{\tau}_{\boldsymbol{k},n}(\boldsymbol{r}) = \frac{1}{\sqrt{N}} \sum_{\boldsymbol{R}_i} e^{i\boldsymbol{k}\cdot\boldsymbol{R}_i} W^{\tau}_n(\boldsymbol{r}-\boldsymbol{R}_i),$$

$$W^{\tau}_n(\boldsymbol{r}-\boldsymbol{R}_i) = \frac{1}{\sqrt{N}} \sum_{\boldsymbol{k}} e^{-i\boldsymbol{k}\cdot\boldsymbol{R}_i} E^{\tau}_{\boldsymbol{k},n}(\boldsymbol{r}),$$

$$\int_{\mathcal{V}} \varepsilon(\boldsymbol{r}) W^{\tau*}_n(\boldsymbol{r}-\boldsymbol{R}_i) W^{\tau'}_{n'}(\boldsymbol{r}-\boldsymbol{R}_j) d^3\boldsymbol{r} = M \delta_{n,n'} \delta_{\tau,\tau'} \delta_{\boldsymbol{R}_i,\boldsymbol{R}_j}. \tag{3}$$

Here N is the total number of "atoms" in the lattice. Let us find the solution of the Eq. (1) in the form

$$\boldsymbol{E}(\boldsymbol{r}) = \sum_{n,\boldsymbol{R}_i,\tau} \mathcal{E}^{\tau}_n(\boldsymbol{R}_i) W^{\tau}_n(\boldsymbol{r}-\boldsymbol{R}_i)\boldsymbol{e}_{\tau}, \tag{4}$$

where $\boldsymbol{e}_{\tau}$ is the unit vector of polarization ($\boldsymbol{e}_1 \perp \boldsymbol{e}_2 \perp \boldsymbol{k}$), $\mathcal{E}^{\tau}_n(\boldsymbol{R}_i)$ is the envelope function of the τ polarization of the electric field. Equation (4) determines the envelope only at the lattice sites $\boldsymbol{R}_i$. To obtain the equation for this value we have to substitute Eq. (4) into Eq. (1), multiply the derived equation by $W^{\tau'*}_{n'}(\boldsymbol{r}-\boldsymbol{R}_j)\boldsymbol{e}_{\tau'}$, and integrate it over $\boldsymbol{r}$. Then we obtain

$$\omega^2 \mathcal{E}^{\tau}_n(\boldsymbol{R}_i) - \sum_{\boldsymbol{R}_j} \mathcal{E}^{\tau}_n(\boldsymbol{R}_j)\Omega_n(\boldsymbol{R}_j-\boldsymbol{R}_i) + \omega^2 \sum_{n',\boldsymbol{R}_j} \mathcal{E}^{\tau}_{n'}(\boldsymbol{R}_j)\mathcal{U}_{n,n'}(\boldsymbol{R}_j,\boldsymbol{R}_i) = 0, \tag{5}$$

where

$$\Omega_n(\boldsymbol{R}_j-\boldsymbol{R}_i) = \frac{1}{N}\sum_{\boldsymbol{k}} \omega^2_{\boldsymbol{k},n} e^{-i\boldsymbol{k}(\boldsymbol{R}_j-\boldsymbol{R}_i)},$$

$$\mathcal{U}_{n,n'}(\boldsymbol{R}_j,\boldsymbol{R}_i) = \frac{1}{N}\int \epsilon(\boldsymbol{r}) W^{\tau*}_{n'}(\boldsymbol{r}-\boldsymbol{R}_j) W^{\tau}_n(\boldsymbol{r}-\boldsymbol{R}_i) d^3\boldsymbol{r}.$$

If we consider the envelope $\mathcal{E}^{\tau}_n(\boldsymbol{r})$ as a smooth function of the position $\boldsymbol{r}$, then this equation can be rewritten as

$$[\Omega_n(-i\nabla) - \omega^2]\mathcal{E}^{\tau}_n(\boldsymbol{r}) - \frac{\omega^2}{M}\sum_{n',\boldsymbol{r}'} \mathcal{E}^{\tau}_{n'}(\boldsymbol{r}')\mathcal{U}_{n,n'}(\boldsymbol{r},\boldsymbol{r}') = 0. \tag{6}$$

Here $\Omega_n(-i\nabla)$ is the Fourier transform of $\Omega_n(\boldsymbol{R}_j-\boldsymbol{R}_i)$, i.e., $\omega^2_{\boldsymbol{k},n}$, after the substitution $\boldsymbol{k} \to -i\nabla$. Note that the equation

$$\mathrm{div}\ \mathcal{E}_n^\tau(\boldsymbol{r}) = \boldsymbol{\nabla}\cdot[\mathcal{E}_n^\tau(\boldsymbol{r})\boldsymbol{e}_\tau] = 0$$

follows from Eqs. (3) and (4).

Equation (6) is the equation for the envelope electric field in the photonic crystal. In contrast to Eq. (1), it does not contain explicitly the terms describing the crystal lattice. The effect of the crystal, in particular its symmetry and material of the "atoms," is described by the term Ω_n, which should be determined numerically. While this term can be expressed via effective parameters: the photonic band gaps and the speeds of light related to the appropriate bands. In our estimations we use the simple model of the photonic band structure considered in the Appendix. Outside the gap region we can assume $\Omega_n(-i\boldsymbol{\nabla}) = -S_n^2\Delta$, where $S_n < 1$ is the speed of light in the nth photonic band.

The interaction $\mathcal{U}_{n,n'}(\boldsymbol{r},\boldsymbol{r}')$ is due to irregularity of the photonic crystal. For the week or smooth irregularity it can be considered as perturbation. This is not the case for the correction to the dielectric permittivity $\epsilon(\boldsymbol{r})$ caused by irregularity [this value is either zero or $\epsilon(\boldsymbol{r}) \sim \varepsilon$]. Additional simplification is possible, if we assume that the Wannier functions $W_n^\tau(\boldsymbol{r}-\boldsymbol{R}_i)$ and $W_{n'}^{\tau',*}(\boldsymbol{r}-\boldsymbol{R}_j)$ overlap only for $\boldsymbol{R}_i = \boldsymbol{R}_j$ and $n = n'$. Then

$$\mathcal{U}_{n,n'}(\boldsymbol{r},\boldsymbol{r}') = \mathcal{U}_n(\boldsymbol{r}),$$

and Eq. (6) turns into the wave equation with the position dependent speed of light.

Note that Eq. (6) does not contain the terms resulting in the light repolarization. This is the consequence of our model, where the optically isotropic crystal has been composed from the isotropic beads. In the more general case, the anisotropy has to be arisen as the result of dependence of $\omega_n(\boldsymbol{k})$ on the wave polarization.

B. Boundary conditions

At first assume $\omega_{\boldsymbol{k},n} = \boldsymbol{S}_n\boldsymbol{k}$, where $\boldsymbol{S}_n$ is the speed of light in the nth photonic band. In the band spectra of real photonic crystals such a relation occurs just apart the band edges.[7] Then $\Omega_n(-i\boldsymbol{\nabla}) = -S_n^2\Delta$, and the Eq. (6), in the absence of interaction, can be written as

$$\left(\Delta + \frac{\omega^2}{S_n^2}\right)\mathcal{E}_n^\tau(\boldsymbol{r}) = 0. \tag{7}$$

Equation (7) permits introduction of the envelope function for the magnetic field $\mathrm{rot}\ \mathcal{E}_n^\tau = i\omega\mathcal{H}_n^{\tau'}$, which obeys the equation

$$\mathrm{rot}(S_n^2\mathrm{rot}\mathcal{H}_n^\tau) - \omega^2\mathcal{H}_n^\tau = 0. \tag{8}$$

Consider scattering of the light wave, the electric field of which is normal to the plane of incidence ($\boldsymbol{E}$ wave). The electric field $\mathcal{E}_n^\tau(\boldsymbol{r})$ satisfies Eq. (7) with $S_n = 1$ in vacuum ($z < 0$). For uniqueness of solution of this equation in the whole space, it is necessary to determine its discontinuity and discontinuity of its normal derivative at the boundary $z = 0$. Artificially it is possible to reduce the symmetry of vacuum to that of the photonic crystal. To obtain the boundary conditions for $\mathcal{E}_n^\tau$, we replace the sharp boundary with some smooth interface where the velocity of light $\boldsymbol{S}_n$ changes continuously from its value in the photonic crystal to that outside it. Then we can choose some region at the interface as a cylinder of small height h. Assuming $h \to a_0 \to 0$ (a_0 is the lattice constant) after integrating of Eq. (7) over this region, we obtain

$$\left[\frac{\partial\mathcal{E}_y}{\partial z}\right] = 0. \tag{9}$$

Square brackets here denote discontinuity of the respective value at the boundary. To obtain the second boundary condition, we have to multiply the Eq. (7) by z before the integration

$$[\mathcal{E}_y] = 0. \tag{10}$$

Boundary conditions for the $\boldsymbol{H}$ wave (the light wave, which electric field is in the incidence plane, hence, the magnetic field is normal to this plane) can be obtained from Eq. (8). The values of $S_n^2\partial\mathcal{H}_y/\partial z$ and $\mathcal{H}_y$ should been continuous at the boundary. Thus,

$$[\mathcal{E}_x] = 0, \tag{11}$$

$$\left[\frac{\varepsilon\omega^2}{q^2}\frac{\partial\mathcal{E}_x}{\partial z}\right] = 0, \tag{12}$$

where q is the z component of the light wave vector.

The boundary conditions we just have obtained mean continuity of the tangent components of the electric and magnetic fields at the interface. In the transmission-reflection problem they lead to the well-known Frensel expressions. These BC hold also for a complicated dispersion law. Indeed, we can expand $\Omega_n(-i\boldsymbol{\nabla})$ in series of $\boldsymbol{\nabla}$, or Δ due to the evenness of $\omega_n(\boldsymbol{k})$. Equations (9) and (10), follow after multiplication of the obtained equations by the relevant power of z and integration over the interface region.

Influence of the omitted term in Eq. (6) is more interesting. If we suppose $\mathcal{U}_{n,n'}(\boldsymbol{r},\boldsymbol{r}')$ as a smooth function of the distance at the interface, then its contribution vanishes after integration. However, this is not the case, if $\mathcal{U}_{n,n'}(\boldsymbol{r},\boldsymbol{r}')$ has a singularity. The origin of this singularity could be interpreted as deviation of the dielectric permittivity from its bulk value at the interface. As the result, Eqs. (9) and (12) accept the form

$$\left[\frac{\partial\mathcal{E}_{ny}^\tau}{\partial z}\right] + \omega^2\left(\alpha\mathcal{E}_{ny}^\tau + \sum_{n'\neq n}\beta_{n,n'}\mathcal{E}_{n'y}^\tau\right) = 0,$$

$$\left[\frac{\varepsilon\omega^2}{q^2}\frac{\partial\mathcal{E}_{nx}^\tau}{\partial z}\right] + \omega^2\left(\alpha\mathcal{E}_{nx}^\tau + \sum_{n'\neq n}\beta_{n,n'}\mathcal{E}_{n'x}^{\tau'}\right) = 0. \tag{13}$$

The same result could been obtained, if we had not supposed $a_0 \to 0$ when integrating of Eq. (7). The rough estimation yields

$$\alpha \sim \frac{a_0}{MS_n^2}\int_{\mathcal{V}}\epsilon(\boldsymbol{r})E_{\boldsymbol{k}n}^{\tau*}(\boldsymbol{r})E_{\boldsymbol{k}n}^\tau(\boldsymbol{r})d^3\boldsymbol{r},$$

$$\beta_{n,n'} \sim \frac{a_0}{MS_n^2}\int_{\mathcal{V}} \epsilon(\boldsymbol{r}) E^{\tau^*}_{\boldsymbol{k}n'}(\boldsymbol{r}) E^{\tau}_{\boldsymbol{k}n}(\boldsymbol{r}) d^3\boldsymbol{r},$$

where $\epsilon(\mathbf{r})$ is difference between $\varepsilon(\boldsymbol{r})$ in the balk of the photonic crystal and that in the first bordering layer. Apparently, $\alpha \lesssim a_0$ and $\beta_{nn'} \lesssim \alpha$.

The second terms in Eq. (13) can be interpreted as an intermediate thin layer at the boundary. Indeed, the boundary conditions (10), (11), and (13), (with $\beta_{n,n'}=0$) relate the electric fields at the interface $z=0$ of two equal medias $z<-d$ and $z>d$ in the presence of thin dielectric layer $-d<z<d$; here $\alpha=2d\delta\varepsilon$, $2d$ is thickness of the layer and $\delta\varepsilon$ is difference of dielectric permittivities of the medias and the layer. This term arises in Eq. (13) because of violation of translational symmetry at the boundary, which concerns mainly the first row of "atoms." Note that small roughness of the boundary also sometimes can be considered as a thin interface layer.[20]

The third terms in Eq. (13) result in interband mixing at the interface that never occurs when the light transmission through the ordinary crystal is considered. They are the terms that determine diffraction of light at the crystal boundary. They mix together all the photonic bands. It is apparent, however, that not all of them are of equal importance. Indeed, the fields of the far remote bands are strongly decaying and so do not affect appreciably the bulk of the crystal. As to the boundary, we can accept there $\mathcal{E}^{\tau}_n(z) \propto \exp(-\kappa_n z)$, so that $\partial\mathcal{E}^{\tau}_n/\partial z = -\kappa_n \mathcal{E}^{\tau}_n$, with the decay exponents $\kappa_n = \sqrt{\pi^2 n^2/a^2 - \omega^2/S_n^2}$ nearly independent of the photon energy for $n \gg \omega a/\pi S_n$. Expressing all these fields via each other, we can rewrite Eq. (13) for only one or a few nearest bands. The new parameters α and $\beta_{n,n'}$ depend on κ_n, but not on the photon energy. Thus, these parameters can be considered as characteristic for the particular boundary.

The Wannier functions Eq. (3) for the photonic states have been introduced in Refs. 13, 14, and 17. It is shown that they can be chosen localized at the lattice site after some unitary transformation.[14] The Wannier function representation has been used to calculate the defect states in photonic crystals. The good agreement with the FDTD simulations has been achieved.[14] The EPA for the Maxwell equations has been developed in Ref. 21. In that paper the envelope was introduced after separation of the slowly and rapidly varying components of the light fields and averaging of the latter. Determination of the envelope function we have used in this paper has been developed in Refs. 13–17. The boundary conditions for the envelopes (9)–(12) have been obtained in Ref. 15. Here we improve these BC by taking into account the discrete character of the photonic crystals ($a_0 \neq 0$).

IV. TRANSMISSION THROUGH THE IDEAL CRYSTAL LAYER. THEORY

Consider the light wave incidence on the photonic crystal localized between the planes $|z|<d$. Let XZ be the plane of incidence, θ and θ_1 are the incident and refraction angles. Omitting the band mixing, we can write the y component of the envelope electric field of the light wave polarized normally to the incidence plane ($\boldsymbol{E}$ wave) as

$$\mathcal{E}_y = e^{i\boldsymbol{k}_{\parallel}x}\begin{cases} e^{ipz} + Re^{-ipz} & \text{if } z<-d, \\ C_1 e^{ikz} + C_2 e^{-ikz} & \text{if } |z|<d, \\ Te^{ipz} & \text{if } z>d, \end{cases} \tag{14}$$

where $\mathcal{E}_y$ belongs to the lower photonic band, if its frequency $\omega < cG/2$, or to the upper photonic band, if $\omega > cG/2$; $\boldsymbol{k}_{\parallel}$ is the parallel to the boundary component of the photon wave vector, $p=\omega\cos\theta$ and $k=(\omega/S)\cos\theta_1 = \omega\sqrt{\varepsilon - \sin^2\theta}$ are the z components of the photon wave vector outside and inside the layer, respectively; k belongs to the appropriate photonic band and it is imaginary, if ω belongs to the photonic gap.

To obtain the coefficients R, C_1, C_2, and T, we have to write BC (10) and (13) (where $\beta_{n,n'}=0$) at both boundaries. This routine leads to the following expression for the transmission coefficient

$$T_p = \frac{4kp}{[i(p-k)+\omega^2\alpha]^2 e^{2ikd} - [i(p+k)+\omega^2\alpha]^2 e^{-2ikd}} \tag{15}$$

or for the transmission rate

$$|T_p|^2 = \frac{16k^2p^2}{Q},$$

where

$$\begin{aligned} Q = {} & [(p-k)^2 + \omega^4\alpha^2]^2 + [(p+k)^2 + \omega^4\alpha^2]^2 \\ & - 2[(p^2 - k^2 + \omega^4\alpha^2)^2 - 4k^2\omega^4\alpha^2]\cos 4kd \\ & - 8k\omega^2\alpha(p^2 - k^2 + \omega^4\alpha^2)\sin 4kd \end{aligned}$$

for the real k and

$$\begin{aligned} Q = {} & [(p-G)^2 + (\omega^2\alpha + \kappa)^2]^2 e^{-4\kappa d} \\ & + [(p+G)^2 + (\omega^2\alpha - \kappa)^2]^2 e^{4\kappa d} \\ & - 2[(p^2 - G^2 + \omega^4\alpha^2 - \kappa^2)^2 - 4(p\kappa + \omega^2\alpha G)^2]\cos 4Gd \\ & - 8(p^2 - G^2 + \omega^4\alpha^2 - \kappa^2)(p\kappa + \omega^2\alpha G)\sin 4Gd, \end{aligned}$$

for the imaginary $k=G+i\kappa$.

The values of arguments of sin and cos ($4kd \sim 4Gd$) are rather large for the thick layers. It is possible to average $|T|^2$ using the equality

$$\frac{1}{2\pi}\int_0^{2\pi} \frac{dt}{a + b\cos t + c\sin t} = \frac{1}{\sqrt{a^2 - b^2 - c^2}}.$$

Then for the real k we obtain

$$\langle |T_p|^2 \rangle = \frac{2kp}{k^2 + p^2 + \omega^4\alpha^2}. \tag{16}$$

Transmission rate at the midgap is determined by the largest of exponents $\exp(4\kappa d)$, so that $|T|^2 \propto \exp(-4\kappa d)$.

The x component of the envelope electric field of the $\mathbf{H}$ wave can be written as

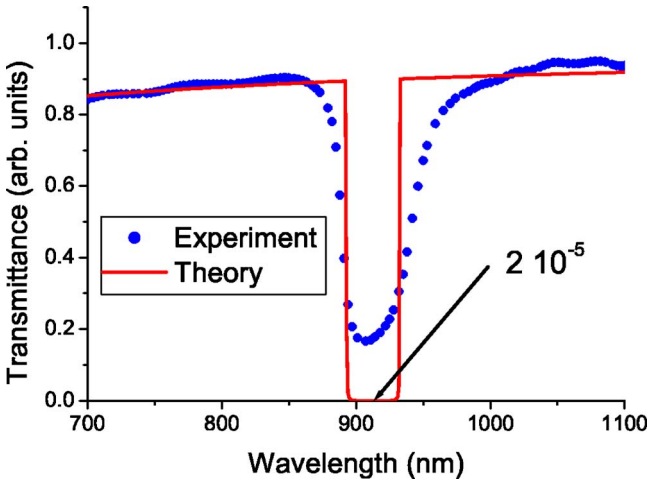

FIG. 2. (Color online) Transparency of a photonic crystal under normal incidence. The theoretical curve corresponds to the model of the perfect crystal.

$$\mathcal{E}_x = e^{i\mathbf{k}_\parallel \mathbf{x}} \cos\theta \begin{cases} e^{ipz} + Re^{-ipz} & \text{if } z < -d, \\ C_1 e^{ikz} + C_2 e^{-ikz} & \text{if } |z| < d, \\ Te^{ipz} & \text{if } z > d. \end{cases} \tag{17}$$

The boundary conditions (11) and (13) yield the transmission coefficient

$$T_s = \frac{2i\varepsilon kpe^{-ipd}}{[\varepsilon^2 p^2 - k^2(i+\alpha p)^2]\sin 2kd + 2\varepsilon kp(i+\alpha p)\cos 2kp},$$

which is equal to Eq. (15) for $\theta=0$. Thus

$$\langle |T_s|^2 \rangle = \begin{cases} \dfrac{2\varepsilon kp}{\varepsilon^2 p^2 + k^2(1+\alpha^2 p^2)} & \text{for real } k, \\ \dfrac{16\varepsilon^2 G^2 p^2 e^{-4\kappa d}}{[(G+\varepsilon p)^2 + \alpha^2 G^2 p^2]^2} & \text{for } k = G + i\kappa, \kappa \ll G, \\ & \text{and } e^{4\kappa d} \gg 1. \end{cases} \tag{18}$$

Mean transmission rate of the nonpolarized light is

$$\langle |T|^2 \rangle = (\langle |T_P|^2 \rangle + \langle |T_S|^2 \rangle)/2.$$

V. TRANSMISSION THROUGH THE CRYSTAL LAYER EXPERIMENT

Figure 2 presents the transmission spectrum of the polystyrene colloid film we have grown (Fig. 1). The close packed fcc crystal has been composed of spherical beads; the diameter of the beads is $D=404$ nm, thus, the lattice constant is $a_0=571$ nm; the thickness of the film is $2d=25$ μm. We have studied the light transmission through the (111) boundary. The transmittance outside the gap has been estimated from Eq. (16), where the value of $\alpha=0.12a_0$ ensures the best fit.

The photonic band structure of the polystyrene close-packed fcc lattice has been calculated in Ref. 22. Position of the dip can be estimated as $\lambda_{\min}=2n_{\text{eff}}d_{111}$, where $d_{111}=D\sqrt{2/3}$ is the body diagonal and n_{eff} is the effective refraction index. We assume[11]

$$n_{\text{eff}}^2 = \epsilon_1 + 3(1-f)\frac{\epsilon_1(\epsilon_2 - \epsilon_1)}{\epsilon_2 + 2\epsilon_1},$$

where $\epsilon_1=2.53$ and $\epsilon_2=1$ are the dielectric permittivities of the polystyrene and vacuum, respectively, $f=0.74$ is the density of fcc packing. Small deviation from this estimation can be explained by the details of the photonic band structure of fcc packing of the polystyrene beads discussed in Ref. 19.

Choosing the gap value Δ from the experiment (Fig. 2), we can estimate transparency of the film from Eq. (A2). The result of this estimation is also presented in Fig. 2 (solid curve); it is of five orders less than the measured value of transparency. Similar results have been obtained also in Refs. 8–10, where the measured values of transparency of the colloid structures have been compared with those obtained after calculation of the photonic band structures from the first principles. Farther in this paper we show that this is the result of disorder of the colloid structures.

VI. TRANSMISSION THROUGH THE NON-IDEAL PHOTONIC CRYSTAL LAYER

In general, the vector potential $\boldsymbol{A}(\boldsymbol{r},t)$ of the light wave obeys the equation

$$\text{rot}\boldsymbol{A}(\boldsymbol{r},t) + \frac{1}{c^2}[\varepsilon(\boldsymbol{r}) + \epsilon(\boldsymbol{r})]\frac{\partial^2 \boldsymbol{A}(\boldsymbol{r},t)}{\partial t^2} = 0. \tag{19}$$

Equation (1) follows from it, if we choose the gauge with the zero scalar potential

$$\boldsymbol{E} = -\frac{\partial \boldsymbol{A}}{\partial t}, \quad \boldsymbol{H} = \text{rot}\boldsymbol{A},$$

and assume $\boldsymbol{A}(\boldsymbol{r},t)=\boldsymbol{A}(\boldsymbol{r})\exp(-i\omega t)$ for the monochromatic light wave. The equality $\boldsymbol{E}=i\omega\boldsymbol{A}$ allows us to introduce the envelope function for the vector potential, which also satisfies Eq. (6).

Let us consider transmittance of light through the photonic crystal located in the region $-d<z<d$. The light wave propagates from $z=-\infty$, so that for the envelope vector potential in the region I ($z<-d$) we can write

$$\boldsymbol{A}(\rho,z) = \boldsymbol{I}e^{i\mathbf{k}_\parallel \rho + ipz} + \int \boldsymbol{R}(k_x,k_y)e^{i\mathbf{k}\rho + iqz}dk_x dk_y$$

and in the region III ($z>d$)

$$\boldsymbol{A}(\rho,z) = \int \boldsymbol{T}(k_x,k_y)e^{i\mathbf{k}\rho + iqz}dk_x dk_y.$$

Here $\boldsymbol{I}$ is the unit vector in the direction of polarization, $\boldsymbol{R}$ and $\boldsymbol{T}$ are the reflection and transmission vectors, ρ, $\boldsymbol{k}$, and $\mathbf{k}_\parallel$ are the coordinate and wave vectors in the XY plane, and $q=\sqrt{\omega^2-\boldsymbol{k}^2}$ and $p=\sqrt{\omega^2-\boldsymbol{k}_\parallel^2}$ are the z components of the wave vectors.

Thus, for the average total transparency we obtain

$$\int \overline{|\boldsymbol{T}(k_x,k_y)|^2}dk_x dk_y = \frac{1}{\Sigma}\int \overline{\boldsymbol{A}(\rho,d)\boldsymbol{A}^*(\rho,d)}d^2\rho.$$

The integrand of this equation is the sum of the diagonal components of the photonic Green function

$D_{ij}(\rho_1,z_1,t_1;\rho_2,z_2,t_2)=-i\langle T\hat{A}_i(\rho_1,z_1,t_1)\hat{A}_j^*(\rho_2,z_2,t_2)\rangle$ (where T means the time ordering). The equation for this function follows from Eq. (6). This is the usual equation for the photonic Green function,[23] where the typical photon dispersion $\omega(\boldsymbol{k})=\boldsymbol{S}\cdot\boldsymbol{k}$ has to be replaced by $\omega_n(\boldsymbol{k})$ from Eq. (2), with the random potential $\mathcal{U}_{n,n'}(\boldsymbol{r}_1,\boldsymbol{r}_2)$ as the perturbation. This allows using the diagrammatic technique to determine the average over the random potential Green function,[23,24] which also should satisfy the boundary conditions (10), (11), and (13). We do not carry out this routine in this paper; instead we consider two simple models of the structure irregularity that are helpful for analyzing of the transmittance spectra.

A. Sort-range irregularities in pseudo-PBG crystals

Position of the midgap is determined by the edge of the Brillouin zone, therefore it depends on the direction in the crystal. The gap width is small in the photonic crystals of the small-index materials. The gap is not absolute in such materials; photon propagation in some direction can be forbidden, but it is not forbidden for the photon of the same frequency in another direction. Such photonic structures are called pseudo-PBG crystals.

If the frequency of light ω belongs to the photonic gap in the direction of the normal $\boldsymbol{n}$ to the crystal boundary $z=0$, then the light propagation in this direction is prohibited. However, midgap position depends on direction in the crystal, and if the gap value is small, then the same ω can be outside the gap in some direction close to $\boldsymbol{n}$. If so, then elastic scattering of the light can increase the in-gap transparency. In this connection, transparency of the thick film depends on the number of scatterers in the decay length $1/\kappa$, but not on the film thickness.

Let us assume the vector potential in the region II ($|z|<d$) as

$$\boldsymbol{A}(\boldsymbol{r})=\boldsymbol{A}_0(\boldsymbol{r})+\boldsymbol{A}_1(\boldsymbol{r}),$$

where $\boldsymbol{A}_0=\boldsymbol{C}_1e^{ik_0z}+\boldsymbol{C}_2e^{-ik_0z}$ is the unperturbed vector potential and $\boldsymbol{A}_1$ is the perturbation caused by irregularity. Then for the zero-range scattering we write

$$\boldsymbol{A}_1(\boldsymbol{r})=f\sum_i \boldsymbol{A}_0(\boldsymbol{r}_i)\frac{e^{ik|\boldsymbol{r}-\boldsymbol{r}_i|}}{|\boldsymbol{r}-\boldsymbol{r}_i|}, \tag{20}$$

where f is a scattering amplitude, we assume it is scalar; $\boldsymbol{r}_i$ are coordinates of the scatterers. We have

$$\frac{e^{ik|\boldsymbol{r}-\boldsymbol{r}_i|}}{|\boldsymbol{r}-\boldsymbol{r}_i|}=\frac{i}{2\pi}\int\frac{e^{i[k_x(x-x_i)+k_y(y-y_i)+q|z-z_i|]}}{q}dk_xdk_y,$$

$$q=\sqrt{\frac{\omega^2}{\varepsilon}-k_x^2-k_y^2}.$$

Hence

$$\int \boldsymbol{A}_1^*(\rho,d)\boldsymbol{A}_1(\rho,d)d^2\rho = f^2\sum_{i,j}\boldsymbol{A}_0^*(\boldsymbol{r}_i)\boldsymbol{A}_0(\boldsymbol{r}_j)\int\frac{e^{i[k_x(x_i-x_j)+k_y(y_i-y_j)+q(z_i-z_j)]}}{q^2}d^2\boldsymbol{k}. \tag{21}$$

Averaging on $\boldsymbol{r}_i$, $\boldsymbol{r}_j$ results in two components. One of them follows from Eq. (21), if $k_x=k_y=0$; it is not interesting for us. The second one arises, if $\boldsymbol{r}_i=\boldsymbol{r}_j$, it yields

$$\int\overline{\boldsymbol{A}_1^*(\rho,d)\boldsymbol{A}_1(\rho,d)}d^2\rho=f^2\sum_i|\boldsymbol{A}_0(\boldsymbol{r}_i)|^2\int\frac{d^2\boldsymbol{k}}{q_z^2}.$$

The integral is equal to $2\pi\ln(\omega/\Delta)$. The sum can be estimated as

$$\sum_i|\boldsymbol{A}_0(\boldsymbol{r}_i)|^2\propto N_i\Sigma\int_0^{2d}e^{-2\kappa z_i}dz_i=\frac{N_i\Sigma}{2\kappa}(1-e^{-4\kappa d}).$$

Thus, contribution of the short-range irregularities to the transparency can be estimated as

$$T_{\mathrm{imp}}=\frac{1}{\kappa L_i}\ln\left(\frac{\omega}{\Delta}\right)(1-e^{-4\kappa d}), \tag{22}$$

where $L_i=(\pi f^2N_i)^{-1}$ is the mean free path.

We see that transmittance is small, if the density of impurities N_i is also small, but it does not contain the exponential factor $\exp(-4\kappa d)$. This is a result of the approximation of low density we have assumed. In the opposite limit we should substitute unperturbed function A_0 in Eq. (20) by its exact value. If we substituted the value of $\boldsymbol{A}_0^*(\boldsymbol{r}_i)\boldsymbol{A}_0(\boldsymbol{r}_j)$ in Eq. (21) by the averaged Green function of the disordered media, then the Eq. (22) would obtain the factor $\exp(-4d/L_i)$. This would also suggest the exponential decay of transmittance, but with a considerably low rate $L_i^{-1}\ll\kappa$. Note that the same factor $\exp(-4d/L_i)$ appears also in the expression for transparency outside the gap, so that it doesn't exist in the peak-to-valley ratio.

Assuming the short-range scattering as the main mechanism limiting the midgap transparency, we can estimate the mean free path as

$$L_i=\frac{2S}{T_{\min}\Delta}\ln\frac{W}{\Delta}, \tag{23}$$

where $T_{\min}$ is the peak-to-valley ratio.

Figure 3 presents results of estimations using this model for the specimen from Fig. 1. We see that short-range irregularity increases the midgap transparency, but does not lead to widening of the dip. The reason is clear. Short-range scattering changes the wave vector of the in-gap photon and, consequently, makes it out-gap. Inverse process, i.e., scattering that changes the wave vector of the out-gap photon and makes it in-gap is improbable for the narrow-gap photonic crystals.

B. Long-range irregularities

Let us consider an imperfect photonic crystal, whose irregularities are due to the smooth structure distortion. Such a

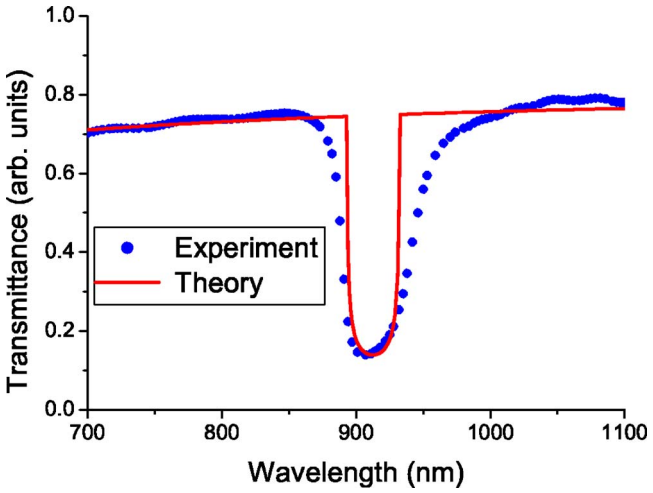

FIG. 3. (Color online) Transparency of a photonic crystal under normal incidence. The theoretical curve corresponds to the model of short-range irregularity.

distortion effectively changes the lattice constant and, therefore, shifts the midgap frequency, which becomes position dependent. As a result, the photon that frequency belong to the gap in the perfect crystal can propagate without attenuation in some regions of the imperfect crystal where the gap position is different. On the other hand, the photon that frequency is outside the gap, but close to it in the perfect crystal propagates with attenuation in some regions of the imperfect crystal where its frequency corresponds to the local gap. Thus, long-range irregularities should lead to widening of the dip in the transparency spectra and increase the midgap transparency.

The light propagation in the structure with long-range irregularities can be described by wave equation with the position-dependent effective speed of light S. The z component of the photon wave vector obeys Eq. (A2) where the photonic band width $W=GS$ is also position dependent. We can write this dependence as $W=W_0(1+\beta\delta f)$, where $\beta\sim 1$ is a constant, and δf is deviation of the density of the cpp packing; this is a random function of the position. This allows us to rewrite Eq. (A2) in the form

$$q(z)=\sqrt{\gamma+\xi(z)},$$

where

$$\gamma=\frac{(\omega^2-W^2)^2-W^2\Delta^2}{4S^2W^2},\ \text{and}\ \xi=-\frac{\omega^2-W_0^2+\Delta^2/2}{S^2}\beta\delta f \tag{24}$$

is also a random function.

The z factor of the envelope function in the WKB approximation contains the exponent

$$J(z)=e^{i\int_0^z[q(z)-q^*(z)]dz}. \tag{25}$$

To average $J(L)$ over $\xi(z)$, let us expand it as

$$\bar{J}=1+i\int_{-d}^{d}\overline{(q_1-q_1^*)}dz_1 - \frac{1}{2}\int_{-d}^{d}\overline{(q_1-q_1^*)(q_2-q_2^*)}dz_1dz_2-\cdots, \tag{26}$$

where $q_1=q(z_1)$, $q_2=q(z_2)$. Third term in this equation can be written as

$$\int_{-d}^{d}\overline{(q_1-q_1^*)(q_2-q_2^*)}dz_1dz_2 = \int_{-d}^{d}\overline{(q_1-q_1^*)(q_2-q_2^*)}dz_1dz_2 + \int_{-d}^{d}(\overline{q_1q_2}-\overline{q_1^*q_2}-\overline{q_1q_2^*}+\overline{q_1^*q_2^*})dz_1dz_2.$$

The last terms $\int_{-d}^{d}\overline{q_1q_2}dz_1dz_2\sim 2dl\overline{q^2}$ (where l is the correlation length; this is the characteristic length of the distortion) are small in comparison with $(\int_{-d}^{d}\overline{q_1}dz_1)^2\sim 4\overline{q^2}d^2$, if $l\ll 2d$. Collecting the first-type terms from each summand of Eq. (26), we obtain

$$\bar{J}=e^{-4\ \mathrm{Im}\,\bar{q}\cdot d}. \tag{27}$$

Obviously, $\mathrm{Im}\,\bar{q}$ should replace $\kappa=\mathrm{Im}\,k$ in expressions (15) and (16).

Assuming the normal distribution of the random value $\xi(z)$, we can evaluate the average $\overline{q(z)}$ as

$$\bar{q}=\frac{1}{\sigma\sqrt{2\pi}}\int_{-\infty}^{+\infty}e^{-\xi^2/2\sigma^2}\sqrt{\gamma+\xi}d\xi,$$

where

$$\sigma^2=\overline{\xi^2}=\frac{(\omega^2-W_0^2+\Delta^2/2)^2}{S^4}\beta^2\overline{\delta f^2}.$$

Then

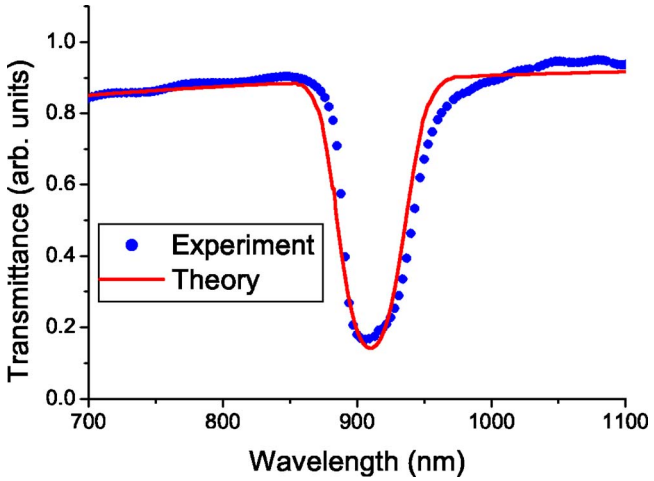

FIG. 4. (Color online) Transparency of a photonic crystal under normal incidence. The theoretical curve corresponds to the model of the long-range irregularity.

$$\mathrm{Im}\,\bar{q}=\begin{cases}\dfrac{\gamma^{3/2}}{4\sqrt{\pi}\sigma}e^{-\gamma^2/4\sigma^2}\left[K_{3/4}\left(\dfrac{\gamma^2}{4\sigma^2}\right)-K_{1/4}\left(\dfrac{\gamma^2}{4\sigma^2}\right)\right] & \text{if } \gamma>0,\\ \dfrac{|\gamma|^{3/2}}{4\sqrt{\pi}\sigma}e^{-\gamma^2/4\sigma^2}\left\{K_{3/4}\left(\dfrac{\gamma^2}{4\sigma^2}\right)+K_{1/4}\left(\dfrac{\gamma^2}{4\sigma^2}\right)+\pi\sqrt{2}\left[I_{3/4}\left(\dfrac{\gamma^2}{4\sigma^2}\right)+I_{1/4}\left(\dfrac{\gamma^2}{4\sigma^2}\right)\right]\right\} & \text{if } \gamma<0.\end{cases} \tag{28}$$

In particular, outside the gap edges ($|\gamma|\gg\sigma$) this estimation yields

$$\mathrm{Im}\,\bar{q}=\begin{cases}\dfrac{\sigma^2}{2\sqrt{2}\gamma^{3/2}}e^{-\gamma^2/2\sigma^2} & \text{if } \gamma>0,\\ \sqrt{|\gamma|}\left(1-\dfrac{\sigma^2}{16\gamma^2}\right) & \text{if } \gamma<0.\end{cases}$$

The factor (27) for positive $\gamma\gg\sigma$ (outside the gap region) is equal to

$$\ln\bar{J}=-\frac{\sigma^2 d\sqrt{2}}{\gamma^{3/2}}e^{-\gamma^2/2\sigma^2}.$$

This means widening of the dip. In the gap region ($\gamma<0$) we obtain decrease of the dip depth. Thus, for the midgap value we obtain the additional factor $\exp[\sigma^2/(4|\gamma|^{3/2})d]$. Rough estimation yields

$$T\sim e^{-4\Delta/S(1-\beta^2\overline{\delta f^2})d}$$

for the midgap transparency and

$$\sqrt{\overline{\delta\lambda_{\min}^2}}\simeq\beta\lambda_{\min}\sqrt{\overline{\delta f^2}}$$

for the mean width of the dip.

To obtain the exact value of transparency, we have to replace $\kappa=\mathrm{Im}\,k$ with $\mathrm{Im}\,\bar{q}$ from Eq. (28) in the expressions (15) and (16). The results of such simulations for the specimen of Fig. 1 are presented in Fig. 4. The best fit corresponds to $\alpha=0.13$, $\beta\sqrt{\overline{\delta f^2}}=0.02$, and $\Delta/W_0=0.02$; the latter is close to the gap value calculated in Ref. 22. From this figure it is clear that the model of long-range irregularity is most appropriate to our experiments.

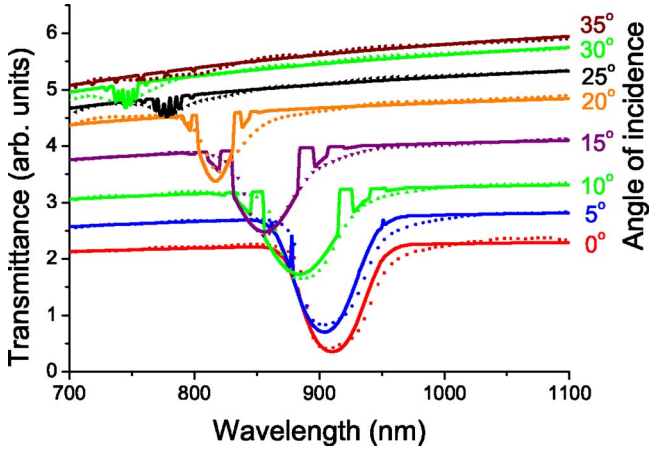

FIG. 5. (Color online) Transparency of an imperfect photonic crystal under oblique incidence. Theoretical curves (solid lines) correspond to the model of long-range irregularity.

Figure 5 presents results of our experiments and simulations for the oblique incident light. Parameters used in simulations are listed in Table I. It is important that α and $\sqrt{\overline{\delta f^2}}$ are the parameters of the structure, which should not depend on the angle of the light incidence. It is apparent from the table that the values of $\alpha=0.14$ and $\beta\sqrt{\overline{\delta f^2}}=0.02$ ensure a good fit with experiments for $\theta<25°$, where the dips are strongly pronounced. Rough estimation of $\beta\simeq 3\epsilon_1|\epsilon_2-\epsilon_1|/[n_{\mathrm{eff}}^2(\epsilon_2+2\epsilon_1)]$ yields $\beta\simeq 0.25$. Thus, mean square deviation of the bead size can be estimated as 4–6%.

It seems that increase of α at $\theta>25°$ is the effect of diffraction, which has not been taken into account in our estimations and which is important at the large incident angles. The reason of oscillations of transparency in the Fig. 5 can be related with inaccuracy of the expansion (24) at $\gamma=0$.

VII. DISCUSSION

The envelope function approach used in this paper permits us to consider the light fields in the perfect photonic crystal as the zero-order approximation. Then distortion of the crystal structure can be considered as perturbation. Simple models we have studied evaluate the result in terms of mean square deviation of the dielectric permittivity $\overline{\delta\varepsilon(\boldsymbol{r})^2}$. In general, diagrammatic approach leads to the more complicated correlators, such as $\overline{\delta\varepsilon(\boldsymbol{r})\delta\varepsilon(\boldsymbol{r}')}$, etc. It is important that all such averages are the statistical parameters of disorder. They should appear in the equation for the average Green function, solution of which directly yields the transmission rate.

TABLE I. Parameters of simulation.

Angle (deg.)	Dip position (nm)	Thickness of intermediate layer α (lattice const)	Mean disorder $\beta\sqrt{\overline{\delta f^2}}$
0	910	0.13	0.0178
5	903	0.15	0.0196
10	884	0.13	0.023
15	856	0.14	0.025
20	817	0.14	0.02
25	778	0.18	0.013
30	743	0.19	0.016
35	757	0.20	0.05

At the boundary of the photonic crystal the envelopes of the light fields must satisfy the boundary conditions, that are more complicated than ones commonly used in optics. Indeed, interaction of light with an individual atom in a common crystal contains a small factor $e^2/\hbar c \approx 1/137$. The effect of this interaction, the dielectric permittivity ε, arises as a result of interaction of light with a large amount of atoms. This allows considering ε as a smooth function of distance from the boundary, that is necessary to derive the commonly used boundary conditions for the electric and magnetic fields.

Interaction of light with an individual "atom" in the photonic crystal is not so small. Therefore, the boundary conditions for the envelope fields should be more complicated. In general, not only the magnetic fields [Eqs. (13)], but also the electric fields can be discontinuous at the boundary. It seems that additional terms have to appear in the equations (10) and (11) for the photonic crystals of the magnetic materials. The form of the boundary conditions depends on the equations for the envelope fields and symmetry of the Bloch functions of the appropriate bands.[25] Similar problem of the boundary conditions for the wave equations at the semiconductor heterojunctions is discussed in Ref. 26.

The boundary conditions (10), (11), and (13) are more general than that used in Ref. 15. The additional terms originate from the first layer of "atoms" where neither Eq. (7) or its vacuum analog with $S_n=1$ hold. Effective thickness of this layer was found to be small $\alpha=0.14a_0$. This is the result of close packing $1-f=0.26 \ll 1$. Indeed, α is zero, if $1-f=0$.

The last terms in Eq. (13) determine diffraction of light at the boundary. Diffraction does not affect essentially transmittance of the photonic crystal layer, because of the exponential factor which essentially determines this value. However, diffraction is very important when the reflection spectra are investigated; these spectra were found to be sensitive to the polarization of the oblique incident light wave.[27] The effect is also sensitive to the boundary roughness.[28]

The reflectivity spectra of the 2D $Al_xGa_{1-x}As$ photonic crystal was studied both experimentally and theoretically in Ref. 29. The theory[29] is based on the scattering matrix method justified in Ref. 30. To ensure the best fit with the experiment, the influence of a thin oxide layer inserted on the surface of the photonic crystal has been taken into account in calculation. It seems that this layer has the same nature as the second terms in Eq. (13).

The simple models of the structure distortion we have considered include the effects of short-range and long-range disorder on the transmittance spectra. It was found that the short-range disorder considerably increases the midgap transmittance, but does not influence the width of the dip. Meanwhile, the long-range disorder causes widening of the dip. In addition, the irregularities of different range demonstrate different dependence of the mid-gap transmittance on the film thickness. The long-range distortion leads to the exponential behavior. This type of irregularity only changes the value of the exponential factor. The short-range distortion can be the reason of the nonexponential behavior; transmittance in this case determines by the thin layer at the boundary where the in-gap photons can turn into the out-gap ones due to the scattering.

In the actual photonic structures the short-range distortion can be associated with the beads of the standard size, which dielectric permittivity is distinguished from the others. The long-range disorder can be caused by the beads of the nonstandard size; distortion of the crystal lattice around such beads relaxes on the large distance.

For the polycrystalline domain structure the influence of the short-range disorder can be connected with light reflection at the domain boundaries (see, e.g., the right part of Fig. 1). In such sense, this is close to the incoherent scattering, which has been observed and explicitly discussed in Ref. 9. We have shown that it does not cause broadening of the dip, but results in significant increase of the midgap transmittance.

The effect of polycrystallinity should depend not only on the size and orientation of the domains, but also on structure of the boundary between them; it is considerable at the sharp boundary, but small at the smooth one. Indeed, exactly solvable models considered in Ref. 31 show that reflectivity of smooth (in comparison with the light wavelength) boundaries is much less than that of the sharp ones.

The long-range disorder in the polycrystalline domain structures can be associated with deviation of the effective speed of light after its refraction into the domain of different orientation. This is the effect that determines the width of the dip.

Influence of disorder on the transmittance and reflectance spectra has been also investigated in Refs. 8, 27, and 32–34. It is established that light propagation becomes diffuse due to scattering at the grain boundaries and point defects. Increase of the midgap transparency due to disorder also has been observed. Simulations of Ref. 8 shows that such increase can not been explained merely by disorder. We suppose this disagreement with our results is due to the difference between our model of disorder and that of Ref. 8. Indeed, certain difference in the exponential indexes can result in considerable difference in the exponential factors. In addition, the authors of Ref. 8 have exploited the one-dimensional model of disorder, which cannot take into consideration the mechanism of short-range scattering discussed in Sec. VI A.

In conclusion, we suggested the envelope functions approach for the electric and magnetic fields of the light wave in the disordered photonic crystals. We used this approximation to investigate the transmittance spectra of imperfect photonic crystals. In particular, we studied the limits of the short-range and long-range irregularity. We found that the short-range disorder cause increase of the midgap transparency, whereas the long-range disorder results in broadening of dips in the transparency spectra.

ACKNOWLEDGMENTS

L.B. appreciates support of the Russian Foundation for Basic Research and the Program for Support of Scientific Schools (Grant No. 4500.2006.2). The work of V.S. has been supported by the TOP NANO 21 Program (Swiss Commission for Technical Innovations, Project No. 5971.2 TNS). V.S. thanks Professor Y. Xia and Dr. J. McLellan (Department of Chemistry, University of Seattle) for a kind intro-

duction to the shear-flow crystallization method.

APPENDIX: SIMPLE MODEL OF PHOTONIC BAND SPECTRUM

Let us suppose the following model of the photonic spectrum in the crystal:

$$\omega^2 = \frac{1}{2}[\omega_1^2 + \omega_2^2 \pm \sqrt{(\omega_1^2 - \omega_2^2)^2 + 4W^2\Delta^2}], \qquad \text{(A1)}$$

where $\omega_1 = S_1|k|$ and $\omega_2 = W - S_2|k|$ are the photonic spectra apart the gap, $W = GS_1$ is the midgap frequency, and Δ is the gap value; the wave vector G corresponds to the appropriate edge of the Brillouin zone: $G = 2\pi/a_0$ for the X point [for (100) boundary] and $G = \pi\sqrt{3}/a_0$ for the L point [for (111) boundary]. From Eq. (A1) it follows

$$\omega_1^2\omega_2^2 - \omega^2(\omega_1^2 + \omega_2^2) + \omega^4 - W^2\Delta^2 = 0.$$

Assuming $\omega_1 = W - qS_1$ and $\omega_2 = W + qS_2$, where $q = G - k \ll G$ at the band edge, we can write

$$[(\omega^2 - W^2)(S_1^2 + S_2^2) + 4W^2S_1S_2]q^2 - 2W(\omega^2 - W^2)(S_1 - S_2)q - [(\omega^2 - W^2)^2 - W^2\Delta^2] = 0.$$

The solutions of this equation are

$$q = \{|(\omega^2 - W^2)(S_1 - S_2)| \pm [(\omega^2 - W^2)^2(S_1 - S_2)^2 + 4S_1S_2[(\omega^2 - W^2)^2 - W^2\Delta^2]]^{1/2}\}/(4WS_1S_2).$$

The module $|(\omega^2 - W^2)(S_1 - S_2)|$ arises here after reducing of $k = G - q$ to the first Brillouin zone. In particular, for $S_1 = S_2 = S$ we obtain

$$q^2 = \frac{(\omega^2 - W^2)^2 - W^2\Delta^2}{2S^2(\omega^2 + W^2)}. \qquad \text{(A2)}$$

*Electronic address: brag@isp.nsc.ru

[1] Y. Lu and Y. Xia, Adv. Mater. (Weinheim, Ger.) **13**, 34 (2001).

[2] D. Amarie, N. Rawlinson, W. Schaich, B. Dragnea, and S. Jacobson, Nano Lett. **5**, 1227 (2005).

[3] P. Sudeep, B. Ipe, K. Thomas, M. George, S. Barazzouk, S. Hotchandani, and P. Kamat, Nano Lett. **2**, 29 (2002).

[4] P. Esfandiari, G. Bernstein, P. Fay, W. Porod, B. Rakos, A. Zarandy, B. Berland, L. Boloni, G. Boreman, B. Lail, B. Monacelli, and A. Weeks, Proc. SPIE **5783**, 470 (2005).

[5] Y. Xia, J. A. Rogers, K. E. Paul, and G. M. Whitesides, Chem. Rev. (Washington, D.C.) **99**, 1823 (1999); V. Shklover and H. Hofmann, in *Handbook of Semiconductor Nanostructures and Nanodevices*, edited by A. A. Balandin and K. L. Wang (American Scientific, Los Angeles, 2005), Vol. 1.

[6] S. G. Johnson and J. D. Joannopoulos, Opt. Express **8**, 173 (2001).

[7] A. Moroz and C. Sommers, J. Phys.: Condens. Matter **11**, 997 (1999); K. Busch and S. John, Phys. Rev. E **58**, 3896 (1998); K. M. Leung and Y. F. Liu, Phys. Rev. Lett. **65**, 2646 (1990); Ze Zhang and Sashi Satpathy, *ibid.* **65**, 2650 (1990); K. M. Ho, C. T. Chan, and C. M. Soukoulis, *ibid.* **65**, 3152 (1990); S. Satpathy, Ze Zhang, and M. R. Salehpour, *ibid.* **64**, 1239 (1990); H. S. Sözüer, J. W. Haus, and R. Inguva, Phys. Rev. B **45**, 13962 (1992).

[8] Yu. A. Vlasov, M. A. Kaliteevski, and V. V. Nikolaev, Phys. Rev. B **60**, 1555 (1999).

[9] V. N. Astratov, A. M. Adawi, S. Fricker, M. S. Skolnick, D. M. Whittaker, and P. N. Pusey, Phys. Rev. B **66**, 165215 (2002).

[10] B. Gates, Y. Lu, Z. Y. Li, and Y. Xia, Appl. Phys. A: Mater. Sci. Process. **76**, 509 (2003).

[11] L. D. Landau and E. M. Lifshitz, *Electrodynamics of Continuous Media* (Pergamon, New York, 1975).

[12] R. J. Spry and D. J. Kasan, Appl. Spectrosc. **40**, 782 (1986); S. A. Asher, P. L. Flaugh, and G. Washinger, Spectroscopy (Amsterdam) **1**, 26 (1986); P. A. Rundquist, P. Photinos, S. Jagannathan, and S. A. Asher, J. Chem. Phys. **91**, 4932 (1989).

[13] O. Painter, K. Srinivasan, and P. E. Barclay, Phys. Rev. B **68**, 035214 (2003).

[14] K. Busch, S. Mingaleev, A. Garcia-Martin, M. Schillinger, and D. Hermann, J. Phys.: Condens. Matter **15**, R1233 (2003).

[15] E. Istrate, M. Charbonneau-Lefort, and E. H. Sargent, Phys. Rev. B **66**, 075121 (2002).

[16] M. Charbonneau-Lefort, E. Istrate, M. Allard, J. Poon, and E. H. Sargent, Phys. Rev. B **65**, 125318 (2002).

[17] J. P. Albert, C. Jouanin, D. Cassagne, and D. Bertho, Phys. Rev. B **61**, 4381 (2000).

[18] S. H. Park, B. Gates, and Y. Xia, Adv. Mater. (Weinheim, Ger.) **11**, 462 (1999).

[19] V. Shklover, Chem. Mater. **17**, 608 (2005); V. Shklover, L. Braginsky, and H. Hofmann, Proc. SPIE **5814**, 239 (2005); V. Shklover, L. Braginsky, and H. Hofmann, Mater. Sci. Eng., C **26**, 142 (2006).

[20] R. Z. Vitlina, A. M. Dykhne, Sov. Phys. JETP **72**, 983 (1991); L. Braginskii, I. Gilinskii, and S. Svitasheva, Sov. Phys. Dokl. **32**, 297 (1987).

[21] C. M. de Sterke and J. E. Sipe, Phys. Rev. A **38**, 5149 (1988).

[22] E. Pavarini, L. C. Andreani, C. Soci, M. Galli, F. Marabelli, and D. Comoretto, Phys. Rev. B **72**, 045102 (2005).

[23] A. A. Abrikosov, L. P. Gor'kov, and I. E. Dzyaloshinskii, *Quantum Field Theoretical Methods in Statistical Physics* (Pergamon, Oxford, 1965).

[24] F. G. Bass and I. M. Fuks, *Wave Scattering from Statistically Rough Surfaces* (Pergamon Press, New York, 1979).

[25] F. López-Tejeira, T. Ochiai, K. Sakoda, and J. Sanchez-Dehesa, Phys. Rev. B **65**, 195110 (2002).

[26] E. L. Ivchenko and G. E. Pikus, *Superlattices and Other Heterostructures* (Springer-Verlang, Berlin, 1997).

[27] J. F. Galisteo-López, F. López-Tejeira, S. Rubio, C. López, and J. Sanchez-Dehesa, Appl. Phys. Lett. **82**, 4068 (2003).

[28] S. Björkert, C. Lopes, Åsa Andersson, and T. Martin, Proc. SPIE **5989**, 292 (2005).

[29] V. N. Astratov, D. M. Whittaker, I. S. Culshaw, R. M. Stevenson,

M. S. Skolnick, T. F. Krauss, and R. M. De La Rue, Phys. Rev. B **60**, R16255 (1999).
[30] D. M. Whittaker and I. S. Culshaw, Phys. Rev. B **60**, 2610 (1999).
[31] A. B. Shvartsburg, P. Hecquet, and G. Petite, J. Opt. Soc. Am. A **14**, 931 (1997).
[32] J. F. Galisteo-López, E. Palacios-Lidón, E. Castillo-Martínez, and C. López, Phys. Rev. B **68**, 115109 (2003).
[33] J. F. Bertone, P. Jiang, K. S. Hwang, D. M. Mittleman, and V. L. Colvin, Phys. Rev. Lett. **83**, 300 (1999).
[34] Y. A. Vlasov, V. N. Astratov, A. V. Baryshev, A. A. Kaplyanskii, O. Z. Karimov, and M. F. Limonov, Phys. Rev. E **61**, 5784 (2000).